

# Instability of Flat Space Enclosed in a Cavity

Maciej Maliborski

*M. Smoluchowski Institute of Physics, Jagiellonian University, 30-059 Kraków, Poland*

(Dated: September 7, 2018)

We consider a spherically symmetric self-gravitating massless scalar field enclosed inside a timelike worldtube  $\mathbb{R} \times S^3$  with a perfectly reflecting wall. Numerical evidence is given that arbitrarily small generic initial data evolve into a black hole.

Bizoń and Rostworowski [1] recently gave evidence that any generic small perturbation of anti-de Sitter (AdS) spacetime evolves into a black hole after a time  $\mathcal{O}(\varepsilon^{-2})$ , where  $\varepsilon$  measures the size of the perturbation. They argued that this instability is a combined result of the following two effects. First, the timelike boundary at spatial infinity of AdS acts as a mirror at which the waves propagating outwards bounce back and return to the bulk. Second, nonlinear resonant interactions of reflected waves tend to shift their energy into increasingly high frequencies, or equivalently increasingly fine spatial scales, which eventually leads to the formation of a horizon. There arises a natural question whether this kind of turbulent dynamics is specific to asymptotically AdS spacetimes, or it can also occur in other situations when dissipation of energy by dispersion is absent. Motivated by this question, in this paper we consider small perturbations of a portion of Minkowski spacetimes enclosed inside a timelike worldtube  $\mathbb{R} \times S^3$ . Admittedly, this problem is somewhat artificial geometrically, yet we think that it sheds some new light on the results of [1].

We restrict ourselves to spherical symmetry and choose a minimally coupled massless scalar field  $\phi(t, r)$  as matter source. It is convenient to parametrize the general spherically symmetric metric as follows

$$ds^2 = -\frac{A}{N^2} dt^2 + A^{-1} dr^2 + r^2 d\Omega^2, \quad (1)$$

where  $r$  is the areal radial coordinate,  $d\Omega^2$  is the round metric on the unit two-sphere, and the functions  $A$  and  $N$  depend on  $t$  and  $r$ . We introduce auxiliary variables  $\Phi := \phi'$  and  $\Pi := A^{-1} N \dot{\phi}$  (hereafter primes and dots denote  $\partial_r$  and  $\partial_t$ , respectively) and write the wave equation  $\nabla^\alpha \nabla_\alpha \phi = 0$  in the first order form

$$\dot{\Phi} = \left( \frac{A\Pi}{N} \right)', \quad \dot{\Pi} = \frac{1}{r^2} \left( r^2 \frac{A\Phi}{N} \right)'. \quad (2)$$

Einstein's equations  $G_{\mu\nu} = 8\pi G [\partial_\mu \phi \partial_\nu \phi - \frac{1}{2} g_{\mu\nu} (\partial\phi)^2]$  take a concise form when expressed in terms of the mass function  $m := \frac{1}{2} r(1 - A)$  (in units where  $4\pi G = 1$ )

$$\frac{N'}{N} = -r (\Phi^2 + \Pi^2), \quad (3)$$

$$m' = \frac{1}{2} r^2 A (\Phi^2 + \Pi^2), \quad (4)$$

$$\dot{m} = r^2 \frac{A}{N} \Phi \Pi. \quad (5)$$

To ensure regularity at  $r = 0$  we require that

$$\Phi(t, r) = \mathcal{O}(r), \quad \Pi(t, r) = p_0(t) + \mathcal{O}(r^2), \quad (6)$$

$$m(t, r) = \mathcal{O}(r^3), \quad N(t, r) = 1 + \mathcal{O}(r^2), \quad (7)$$

with expansion coefficients uniquely determined by a free function  $p_0(t)$ . We set  $N(t, 0) = 1$  so that  $t$  is the proper time at the center.

In the asymptotically flat situation the above system has been extensively studied in the past leading to important insights about the dynamics of gravitational collapse. In particular, Christodoulou showed that for small initial data the fields disperse to infinity [2], while for large initial data black holes are formed [3]. The borderline between these two generic outcomes of evolution was explored numerically by Choptuik leading to the discovery of critical phenomena at the threshold of black hole formation [4]. The aim of this note is to see how these findings are affected by placing a reflecting mirror at some finite radius  $r = R$ . In other words, instead of asymptotically flat boundary conditions, we consider the interior Dirichlet problem inside a ball of radius  $R$  with the boundary condition  $\Pi(t, R) = 0$ . The Dirichlet boundary condition and the requirement of smoothness imply that the coefficients of the power series expansions at  $r = R$  (here  $\rho = 1 - r/R$ )

$$\phi(t, r) = \sum_{k \geq 1} \phi_k(t) \rho^k, \quad (8)$$

$$N(t, r) = \sum_{k \geq 0} N_k(t) \rho^k, \quad m(t, r) = \sum_{k \geq 0} m_k(t) \rho^k$$

are determined recursively by  $\phi_1(t)$ ,  $N_0(t)$ , and  $m_0(t)$ . For example, at the lowest order we have:

$$2\phi_2(t) - \left( 1 + \frac{R}{R - 2m_0(t)} \right) \phi_1(t) = 0. \quad (9)$$

Taken at  $t = 0$ , the expansions (8) express the compatibility conditions between initial and boundary values. It follows immediately from equation (5) that  $m_0(t) = M = \text{const}$ , where  $M$  is the total energy. From (4) the total energy can be expressed as the volume integral

$$M = \frac{1}{2} \int_0^R A (\Phi^2 + \Pi^2) r^2 dr. \quad (10)$$

We solved the initial-boundary value problem for the system (2)-(5) numerically using the method of lines

with a fourth-order spatial finite-difference discretization scheme. Time integration of evolution equations was performed with use of an adaptive, explicit Runge-Kutta-Dormand-Prince algorithm of order 5(4). The metric functions were updated by solving the slicing condition (3) and the Hamiltonian constraint (4). The degree to which the constraint (5) is preserved and the mass (10) is conserved depending on the spatial resolution was used to verify the fourth order convergence of the numerical scheme. Let us point out that this fully constrained evolution scheme is very efficient computationally and easy to make parallel because the update of metric functions reduces to simple integrations. Namely, from (3) we have

$$\log N(t, r) = - \int_0^r s [\Phi(t, s)^2 + \Pi(t, s)^2] ds, \quad (11)$$

and from the combination of (3) and (4) we get

$$A(t, r) = \frac{N(t, r)}{r} \int_0^r \frac{ds}{N(t, s)}. \quad (12)$$

Numerical results presented below were generated from Gaussian-type initial data of the form (without loss of generality we set  $R = 1$ )

$$\Phi(0, r) = 0, \quad \Pi(0, r) = \varepsilon \exp\left(-32 \tan^2 \frac{\pi}{2} r\right). \quad (13)$$

These initial data vanish exponentially as  $r \rightarrow 1$  so compatibility conditions are not an issue. The results are very similar to those of [1], as can be seen by comparing Figs. 1 and 2 with the analogues figures in [1]. For large amplitudes the evolution is not affected by the mirror; the wave packet rapidly collapses, forming an apparent horizon at a point where the metric function  $A(t, r)$  goes to zero. However, a wave packet which is marginally too weak to form a horizon on the first implosion, does so on the second implosion after being reflected back by the mirror. As in the AdS case, this leads to a sequence of critical amplitudes  $\varepsilon_n$  for which the solutions, after making  $n$  bounces, asymptote Choptuik's critical solution (see Fig. 1). To track the steepening of the wave packet for very small amplitudes, we follow [1] and monitor the Ricci scalar at the center  $R(t, 0) = -2\Pi(t, 0)^2$ . This function oscillates with approximate period 2. Initially, the amplitude stays almost constant but after some time it begins to grow exponentially and eventually a horizon forms [see Fig. 2(a)]. As shown in Fig. 2(b), the time of onset of exponential growth  $T$  scales with the amplitude of initial data as  $T \sim \varepsilon^{-2}$ , which indicates that arbitrarily small perturbations (for which it is impossible numerically to track the formation of a horizon) eventually start growing.

In [1] the numerical results were corroborated by a non-linear perturbation analysis which demonstrated that the instability of AdS is caused by the resonant transfer of energy from low to high frequencies. For the problem

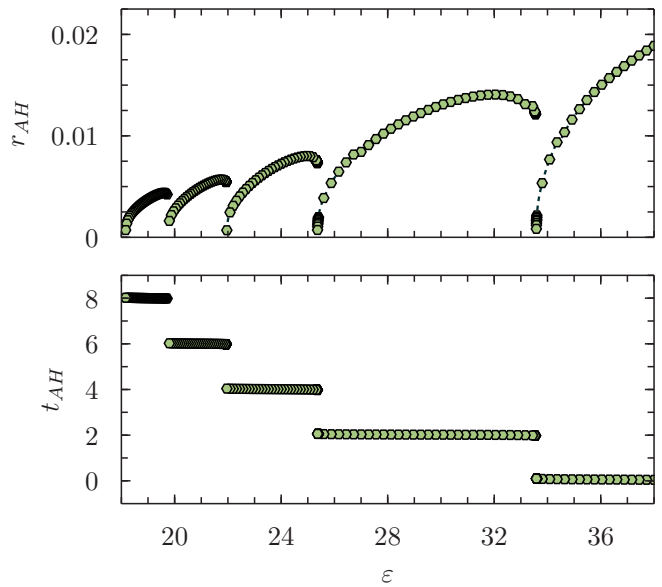


FIG. 1: Apparent horizon radius  $r_{AH}$  (top) and corresponding formation time  $t_{AH}$  (bottom) as a function of the amplitude of initial data (13). At critical points  $\lim_{\varepsilon \rightarrow \varepsilon_n^+} r_{AH}(\varepsilon) = 0$ , while the horizon formation time exhibits jumps of size  $t_{AH}(\varepsilon_{n+1}) - t_{AH}(\varepsilon_n) \approx 2$  (time in which the pulse traverses the cavity back and forth).

at hand, the evolution of linearized perturbations is governed by the free radial wave equation  $\ddot{\phi} = r^{-2}(r^2\phi)'$ ; hence the eigenfrequencies and eigenmodes are

$$\omega_j^2 = \left(\frac{j\pi}{R}\right)^2, \quad e_j(r) = \sqrt{\frac{2}{R}} \frac{\sin \omega_j r}{r}, \quad j \in \mathbb{N}. \quad (14)$$

As in AdS, the spectrum is fully resonant (that is, the frequencies  $\omega_j$  are equidistant), so the entire perturbation analysis of [1] can be formally repeated in our case. We say 'formally' because, in contrast to the AdS case, the eigenmodes (14) violate the compatibility conditions at  $r = R$  and therefore they cannot be taken as smooth initial data.

The transfer of energy to higher modes (which is equivalent to the concentration of energy on smaller scales) can be quantified by monitoring the energy contained in the linear modes  $E_j = \Pi_j^2 + \omega_j^{-2}\Phi_j^2$ , where  $\Phi_j = (A^{1/2}\Phi, e_j')$  and  $\Pi_j = (A^{1/2}\Pi, e_j)$ , with the inner product defined as  $(f, g) := \int_0^R f(r)g(r)r^2 dr$ . Then, the total energy can be expressed as the Parseval sum  $M = \sum_{j=1}^{\infty} E_j(t)$ . The evidence for the energy transfer is shown in Fig. 3 which depicts a Sobolev-type weighted energy norm  $\tilde{E}(t) = \sum_{j=1}^{\infty} j^2 E_j(t)$ . The growth of  $\tilde{E}(t)$  in time means that the distribution of energy shifts from low to high frequencies. The characteristic staircase shape of  $\tilde{E}(t)$  indicates that the energy transfer occurs mainly during the subsequent implosions through the center. This observation leads to the conclusion that the only role of the mirror is to reflect the pulse so that it can be focused

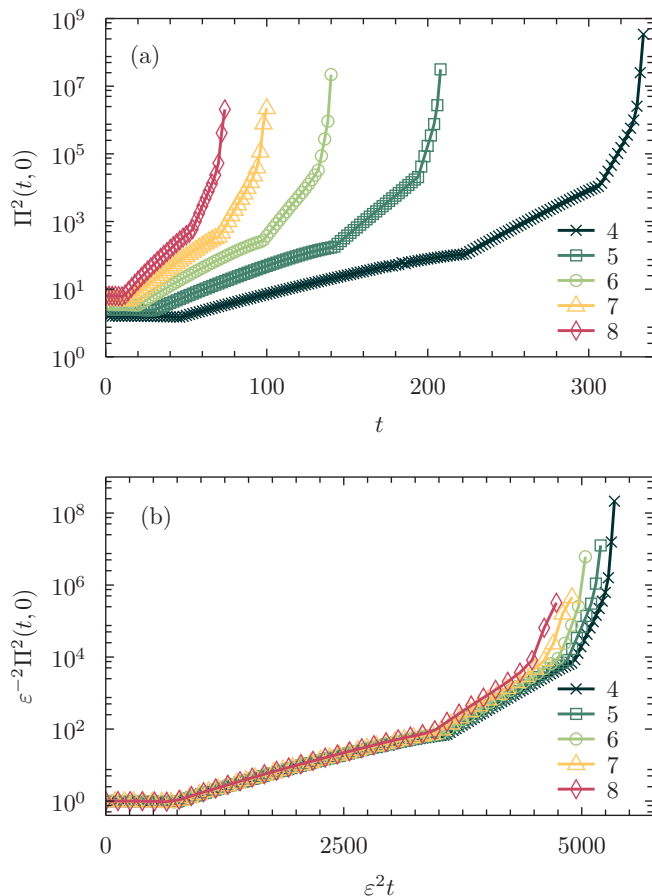


FIG. 2: (a) The function  $\Pi^2(t, 0)$  for solutions with initial data (13) for several moderately small amplitudes. For clarity of the plot only the envelopes of rapid oscillations are depicted. (b) The curves from the plot (a) scaled according to  $\epsilon^{-2}\Pi^2(\epsilon^2 t, 0)$ . Plotted curves are labelled by the value of initial data amplitude  $\epsilon$ .

during the next implosion.

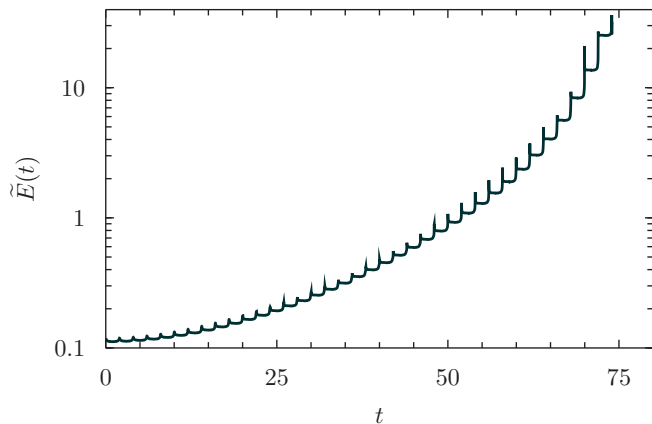


FIG. 3: Plot of the weighted energy norm  $\tilde{E}(t)$  for the solution with initial amplitude  $\epsilon = 8$ . The steep bursts of growth occur when the pulse implodes through the center.

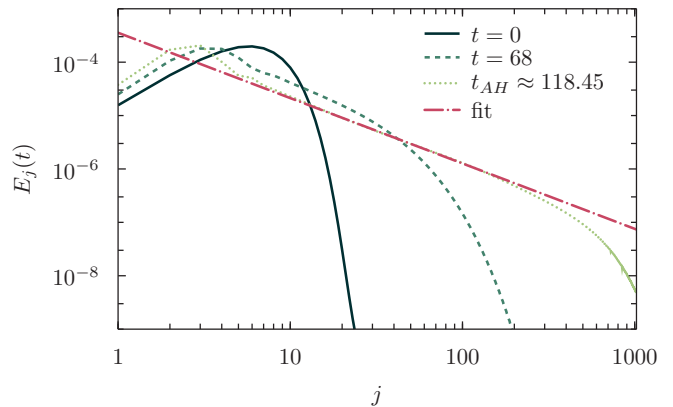


FIG. 4: Energy spectra at three moments of time (initial, intermediate, and just before collapse) for the solution with initial amplitude  $\epsilon = 6$ . The fit of the power law  $E_j \sim j^{-\alpha}$  performed on the interval  $j \in [16, 128]$  gives the slope  $\alpha \approx 1.2$ .

Another aspect of the turbulent cascade is shown in Fig. 4 which depicts the spectrum of energy (that is, the distribution of the total energy over the linear modes) for the solution with initial data (13) and  $\epsilon = 6$ . Initially, the energy is concentrated in low modes; the exponential decay of the spectrum expresses the smoothness of initial data. During the evolution the range of excited modes increases and the spectrum becomes broader. Just before horizon formation an intermediate range of the spectrum exhibits the power-law scaling  $E_j \sim j^{-\alpha}$  with exponent  $\alpha = 1.2 \pm 0.1$ . Energy spectra in evolutions of different families of small initial data exhibit the same slope (up to a numerical error) which indicates that the exponent  $\alpha$  is universal. We note that the power-law spectrum with a similar exponent was also observed in the AdS case [5]. As pointed out in [1], the black hole formation provides a cut-off for the turbulent energy cascade for solutions of Einstein's equations (in analogy to viscosity in the case of the Navier-Stokes equation). It is natural to conjecture that the power-law decay is a consequence of the loss of smoothness of the solution during collapse; however we have not been able to compute the exponent  $\alpha$  analytically.

Close parallels between the results presented in this work and [1, 6] indicate that the turbulent behavior is not an exclusive domain of asymptotically AdS spacetimes but a typical feature of 'confined' Einstein's gravity with reflecting boundary conditions. This answers the question about the role of the negative cosmological constant  $\Lambda$  posed at the end of [1]: the only role of  $\Lambda$  is to generate the timelike boundary at spatial and null infinity.

Finally, let us point out that instead of the Dirichlet condition at the boundary of the cavity  $\Pi(t, R) = 0$  one can alternatively consider the Neumann boundary condition  $\Phi(t, R) = 0$  (for which the energy flux through the boundary vanishes as well). In the Neumann case the

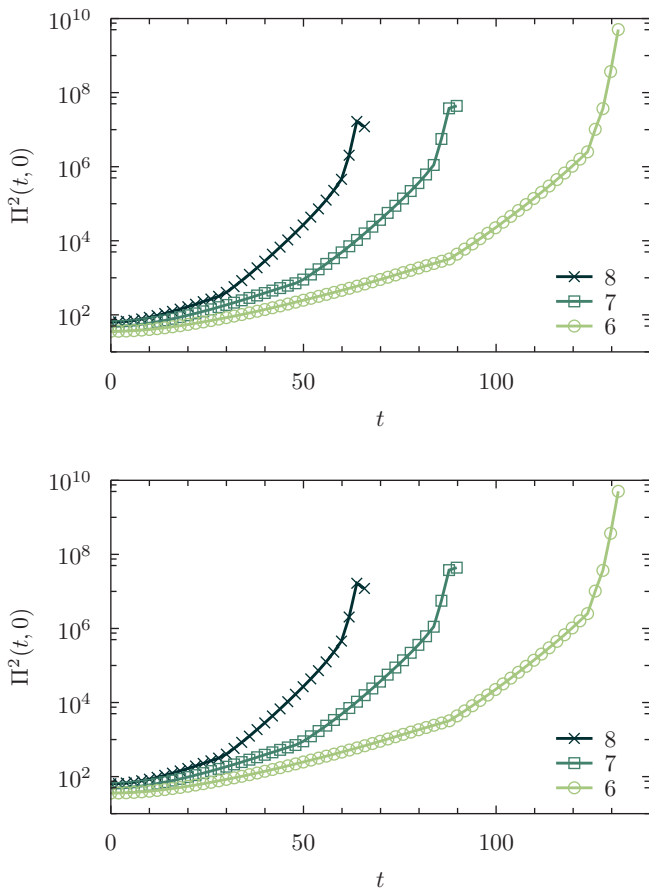


FIG. 5: The analogue of Fig. 2 for the Neumann boundary condition [for the same initial data (13)]. The time of apparent horizon formation exhibits the same type of scaling  $t_{AH} \sim \varepsilon^{-2}$ .

eigenfrequencies of the linearized problem, determined by the condition  $\tan R\omega_j = R\omega_j$ , are only asymptotically resonant

$$\omega_j = \frac{\pi}{R} \left( j + \frac{1}{2} \right) + \mathcal{O}(j^{-1}), \quad j \rightarrow \infty, \quad j \in \mathbb{N}$$

nonetheless numerical simulations show similar turbulent behavior as in the Dirichlet case (see Fig. 5). This indicates that the spectrum of linearized perturbations need not be fully resonant for triggering the instability (cf. Ref. [7] for an opposite conclusion based on the nonlinear perturbation analysis).

I thank Piotr Bizoń and Andrzej Rostworowski for suggesting the problem, encouragement, and discussions. This work was supported in part by the NCN Grant No. NN202 030740 and Dean's Grant No. DSC/000703. Most computations were performed on the supercomputer Deszno at the Institute of Physics of the Jagiellonian University.

- 
- [1] P. Bizoń and A. Rostworowski, *Phys. Rev. Lett.* **107**, 031102 (2011).
  - [2] D. Christodoulou, *Comm. Math. Phys.* **105**, 337 (1986).
  - [3] D. Christodoulou, *Comm. Math. Phys.* **109**, 613 (1987).
  - [4] M.W. Choptuik, *Phys. Rev. Lett.* **70**, 9 (1993).
  - [5] P. Bizoń and A. Rostworowski (private communication).
  - [6] J. Jałmużna, A. Rostworowski, and P. Bizoń, *Phys. Rev. D* **84**, 085021 (2011).
  - [7] O.J.C. Dias *et al.*, arXiv:1208.5772.

